

Interactive and Procedural Modeling of Featured Chinese Architectures

Chun-Yen Huang¹(✉), Yang-Siu Sheng¹, and Wen-Kai Tai²

¹ Department of Computer Science and Information Engineering,
National Dong Hwa University, Hualien 97441, Taiwan
nschuang.tw@gmail.com, asdzxc123g@gmail.com

² Department of Computer Science and Information Engineering,
Nation Taiwan University of Science and Technology, Taipei, Taiwan
wenkaitai@gmail.com

Abstract. The traditional Chinese garden contains many types of tings, corridors, walls, etc. For artists, it is tedious work to model these kinds of featured Chinese architecture due to the strict and complex construction rules. We propose an interactive and procedural tool to modeling featured Chinese architectures that appear in the Chinese garden. Based on the previous research about modeling basic structures of Chinese architecture, we extend to model more featured Chinese architectures, such as double-eave ting, combined ting, corridor, and wall effectively and efficiently, and combine them into a complete Chinese garden. By adjusting the overlapped components, we can combine two single tings into a combined ting. By modifying ting's structure, we can construct a variant of corridors or garden walls upon few input parameters. In addition, the result 3D model can be exported in different LODs, making the use of the model more practicable and flexible. As experimental results shown, complex 3D models of a Chinese garden with several different featured Chinese architectures can be created in minutes.

Keywords: Ting · Corridor · Garden wall · Chinese pavilion · Procedural modeling · Interactive modeling · Chinese architecture · Chinese garden

1 Introduction

Featured Chinese architectures, such as ting, palace, and pagoda, have been becoming increasingly significant in the fields of cultural heritage preservation, restoration of ancient civilization, and digital entertainment with their complex structure and decoration. However, the strict rules of proportions in traditional construction of featured Chinese architectures [1–3] make it too complex to construct using a number of simple grammars (grammar-based approach) and sketches (sketch-based approach). Huang and Tai [4] proposed a method to modeling ting by exploring the parameter relationships and summarizing them in association with two principal parameters.

In this paper, we extend the method Huang and Tai [4] to modeling more types of featured Chinese architectures structure: (1) extended roof structures, such as

gable-and-hip roof, double-eave structure, and pagoda, and (2) extended ting structure, such as combined ting, corridor, and garden wall, with the level-of-detail technique to reduce the number of polygon used of the resultant 3D model. It is more practicable and flexible to use in various applications of virtual Chinese architectures, such as digital content industries, including computer/video games, animations, and movies.

The rest of this paper is organized as below. In Sect. 2, we briefly review the related work on procedural modeling approaches. Section 3 gives an overview of the featured Chinese architecture's structures. Section 4 specifies the extended approach of the featured Chinese architectures. The simplification & Level-of-Detail will be described in Sect. 5. In Sect. 6, the experimental results are shown. Finally, we conclude with a discussion about future work in Sect. 7.

2 Related Work

Procedural modeling approaches [4, 6] allow users to produce a high degree of complexity with, relatively speaking, a few simple inputs. For increasing the variations of the results, more control parameters need to be added to the procedure. However, it would be complex and less intuitive for users to predict the effects by adjusting particular parameters and the combinations of the parameters as the number of input parameters grows.

Some recent work in architecture modeling is based on grammars. The approaches based on L-systems [7–10] have achieved impressive results on branching objects such as plants and streets. Even so, there are numerous types of buildings that are constructed with quite different structures from branching objects.

Shape grammar is a powerful modeling tool. Wonka et al. [11] proposed split grammars that allow automatic derivations are useful for various building styles. Müller et al. [12] introduced CGA shape, which extends the split grammars. Müller et al. [13] proposed a specialized generation rule for reconstructing Puuc-style architecture at Xkipché in Mexico based on CGA Shape. Bokeloh et al. [14] proposed an inverse procedural modeling approach that analyzes the input 3D model to build a shape grammar and synthesizes a similar one with the assistance of the user's interactions. Nevertheless, still, there are revelations of insufficient reasons for the method to support curved surface due to the restrictions of CGA shape.

Another method to modeling architectures is the sketch-based approach. Chen et al. [15] proposed a system of freehand sketch-based modeling of architectures. The system periodically interprets its 2.5D-geometry as the sketch has been drawn by users. However, drawing the sketches of architecture for novice users is difficult. As a result, it is even harder to produce a correct projection concept. We take advantage of the previous approach [4], which created an initial frame of feature Chinese architecture for users to adjust the shapes in the directions they wish rather than starting from nothing, and extend it for more types of featured Chinese architecture.

3 Featured Chinese Architectures in a Chinese Garden

Referring to the construction guides of ancient featured Chinese architecture [1–3], a Chinese garden is composed by several featured Chinese architectures. These architectures come in several types, such as ting, palace, and pagoda, are majorly classified by the roof types. These basic roof types are: round, pyramidal, hollow, hip, gable, overhanging-gable, gable-and-hip, round-ridge, and helmet types as shown in Fig. 1. The hip, gable, overhanging-gable, gable-and-hip, and round ridge types only appear on the rectangular platform.

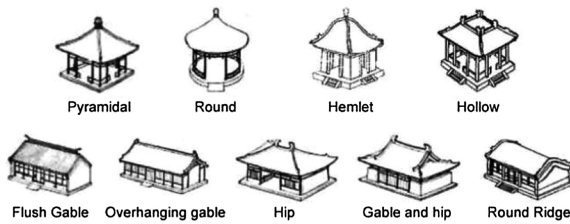


Fig. 1. The nine roof types

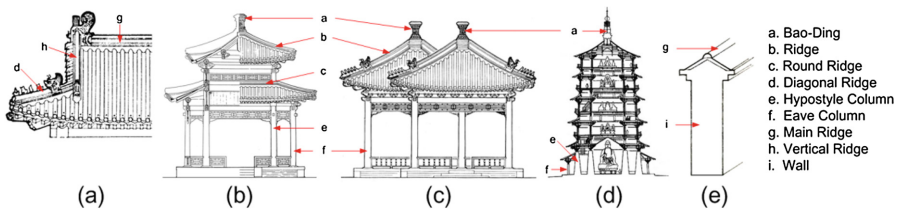


Fig. 2. Exemplar structures of (a) A left-half gable-and-hip roof in front-view, (b) A double-eave, (c) A combined ting, (d) A pagoda, and (e) A garden wall.

Figure 2 shows exemplar structures of the gable-and-hip roof, double-eave, combined ting, pagoda, and garden wall. Figure 2(a) shows a half gable-and-hip roof in front-view. Double-eave structure means there is an extra eave as a veranda around the main structure, below the main roof of the building [3], as shown in the Fig. 2(b). A combined ting structure is shown in Fig. 2(c); it is combined by two single tings. The structure of Pagoda is shown in Fig. 2(d), and usually stacks three or more layers [1]. The overall size of each layer decreases from bottom to top. Figure 2(e) shows the structure of a garden wall. A garden wall is assembled by a gable roof and a solid wall. The structure of a corridor is the same as a single ting.

4 Chinese Garden Architectures Modeling

The previous work [4] is improved to model gable-and-hip roof, double-eave ting, and pagoda, and extended ting structures: combined ting, corridor, and garden wall. In this Section, we specify the methods for modeling these structures. Figure 3 shows the structural frame and control points we use.

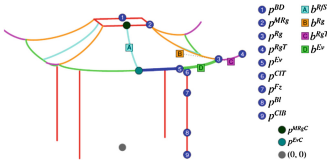


Fig. 3. An illustration for control points on a structure frame. The blue dots show the position control points PCPs, and the bending control points BCPs are shown in colored squares. Additionally, the blue line shows the straight part of the eave while the green curve shows the curved part of the eave. (Color figure online)

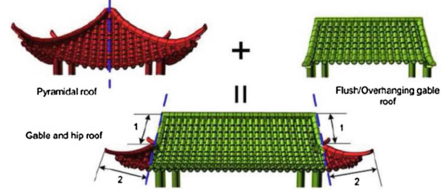


Fig. 4. An illustration of the combination of gable-and-hip roof. The red part of the gable-and-hip roof is from the pyramidal roof, while the green part is from the overhanging roof. (Color figure online)

4.1 Extended Roof Structures

Gable-and-hip Structure. Gable-and-hip roof can be considered as a combination of the pyramidal and overhanging roof. Figure 4 shows an illustration of the concept of this combination. Therefore, we construct the frame of gable-and-hip roof by editing the pyramidal roof on a rectangular ting as shown in Fig. 5.

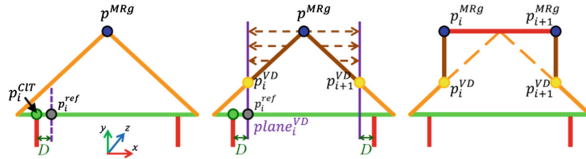


Fig. 5. An illustration in front view of creating the frame of a gable-and-hip roof. The purple lines indicate the plane $plane_i^{VD}$ obtain by a reference point p_i^{ref} of the corresponded columns' position p_i^{CIT} . The red, brown, orange, and green lines represent the main-ridge, vertical ridges, diagonal ridges, and eave line, respectively. (Color figure online)

Given a segmented single ridge curve in the frame of a pyramidal structure (orange curve on the left of Fig. 3), we first decide the position of the joint point p^{VD} between

the vertical ridge (legend h in Fig. 2) and the diagonal ridge (legend d in Fig. 2) on the original ridge as shown on the middle of Fig. 5. To help us deciding the position of the joint point p^{VD} , we need a reference point p_i^{ref} , as shown on the left of Fig. 5, whose initial position is set to be $p_i^{ref} = p_i^{CIT} - (D, 0, 0)$ [1]. Thus, the i^{th} joint point p_i^{VD} can be decided as the intersection point of the i^{th} ridge and a plane $plane_i^{VD}$ as default position, where the plane $plane_i^{VD}$ shown by the purple line on the middle of Fig. 5 is defined by the reference point p_i^{ref} and x -axis. Then, the segment points from p_i^{VD} to p_i^{MRg} on the original ridge are projected to $plane_i^{VD}$ to create the vertical ridge (brown lines at the right of Fig. 5). Afterward, the frame of the main ridge is created by $\overline{p_i^{MRg} p_{i+1}^{MRg}}$. The rest of the frames, PCPs and BCPs of the body and the platform are the same as the pyramidal ting.

User can adjust the position of p_i^{VD} by moving the PCP p_i^{MRg} along $\overline{p_i^{MRg} p_{i+1}^{MRg}}$ horizontally to obtain the different length ratio between the vertical and diagonal ridges on the original ridge.

Double-eave Structure. The double-eave structure is modeled by assembling a shorter hollow roof structure to a taller structure. The length of the hollow roof's main ridge corresponds to the width or depth of the taller structure.

For a given basic structure as the lower part of the double-eave structure, we first change the roof type to hollow roof for adding the upper structure. The main ridge length in width and depth direction are set to be $width - 2x$ and $depth - 2x$, respectively, where x is raising step [4], to fit the upper structure [3]. We then take the ratio of original to the adjusted width/depth to decrease the scale the upper structure.

Double-rounding. Figure 6 shows two kinds of column layout in the double-eave structure: single-rounding and double-rounding [3]. As the double-rounding column structure shown in Fig. 6(a), the columns of the upper structure (orange dots) extend to the lower platform, which become hypostyle columns.

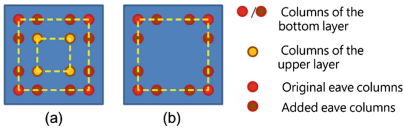


Fig. 6. The top-view of the two column layouts: (a) double-rounding column structure, and (b) single-rounding column structure. (Color figure online)

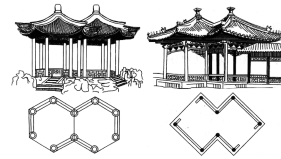


Fig. 7. The structures and layouts of an edge-aligned and a ridge-aligned combined ting.

Single-rounding. In the opposite, if the columns of the upper structure do not extend to the platform, it is called the single-rounding column structure as shown in Fig. 6(b). Therefore, as to the double-rounding structure, we set the column's height to $1.8 \times (\text{original column height})$; as to the single-rounding structure, we set the

column's height to $0.4 \times (\text{original column height})$ with the upper structure be lifted $1.4 \times (\text{original column height})$.

The diameter of the hypostyle column is $D + 1$, where D is the diameter of the eave column [2]. Finally, for each eave column, two more extra eave columns are added along the width and depth direction with an offset distance x inward as shown in Fig. 6(b).

Pagoda Structure. We stack multiple layers in y direction and scale down the size (in our implementation, 0.75) of each layer from bottom to top to model the pagoda. Same as double-eave structure, the roof type of the lower layers except the top layer is set to be the hollow roof, which the length of the hollow roof's main ridge is equal to the corresponding width or depth of the upper layer structure.

4.2 Extended Ting Structures

The following subsections introduce the extended ting structures, including combined ting and corridor and garden wall.

Combined Ting Structure. The width, depth, platform shape, and roof type of the two single tings should be the same when combining these two single tings to a combined ting [18, 19]. As described in [3, 16], there are two kinds of alignment structure when combining two single tings: edge-aligned structure, as shown in the left of Fig. 7, and ridge-aligned structure, as shown in the right of Fig. 7. Also, for symmetry, combining different roof types should be limited to the following rules:

- (1) **Pyramidal and Hollow** - can be combined by edge-aligned or ridge-aligned structures.
- (2) **Gable and Hip** - can be combined only by edge-aligned structure.

Accordingly, we can obtain a combined ting by the following steps: (1) align two tings with the edge/ridge, (2) decide the distance between the centers of the two tings, (3) calculate the intersected plane, and (4) process the intersected region. The first two steps are straight forward, so the following describes the details of the last two steps.

Intersected Plane Calculation. Two aligned tings $ting_A$ and $ting_B$ can be regarded as been mirrored from one to another by a mirror plane. This plane can be considered as the intersection plane $plane^M$ which lies in the middle of $\overline{p_A^{BD} p_B^{BD}}$ with its normal parallels to $\overline{p_A^{BD} p_B^{BD}}$ as shown in the left of Fig. 8. Thus, the distance d_{plane^M} from p^{BD} to $plane^M$ will be less than $\|\overline{p^{BD} p^{EvC}}\|$ (edge-aligned) or $\|\overline{p^{BD} p^{Rg}}\|$ (ridge-aligned).

Intersection Processing. After obtaining the intersected plane $plane^M$, we can place the two same ting $ting_A$ and $ting_B$ along $\overline{p_A^{BD} p_B^{BD}}$ at the distance of $2d_{plane^M}$ to obtain the combined ting. However, there are several components and tiles will be intersected to each other when combining these two single tings. Therefore, we have to deal with these intersected components and tiles to obtain a complete single combined ting.

Body Structure. According to the description in [4], the rest of PCPs can be calculated as soon as the column bottom control point p^{CIB} has been decided. Thus, we have to adjust the p^{CIB} first for processing the intersection. The p_i^{CIB} that underneath the interior area of the other roof should be move to the intersected plane $plane^M$ along the edge towards p_{i+1}^{CIB} (rectangle ting) or p_{i-1}^{CIB} (otherwise, if p_{i+1}^{CIB} is still at the same side of p_i^{CIB}) as shown in the left of Fig. 8. The rest of the components of the body structure are adjusted accordingly as stated in [4].

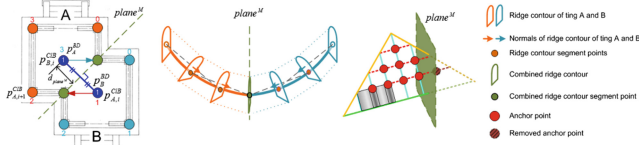


Fig. 8. An illustration of intersected plan calculation and intersection processing. Left: the top view of a ridge-align combined ting. Calculate the intersected plane $plane^M$ by the blue reference line defined by $\overline{p_A^{BD}p_B^{BD}}$, and then move the column bottom control point lies at the opposite side of $plane^M$ (related to p^{BD}) back onto the $plane^M$. Middle: adjust the ridge contours onto the intersected plane $plane^M$. Right: remove the anchor points that lie at the opposite side of $plane^M$ (related to p^{BD}). (Color figure online)

Roof Structure. For the ridges, since the 3D model of ridges is generated by sweeping [4], we adjust the last slice of the model of one ting onto the intersected plane to be connected to the other ting as shown in the middle of Fig. 8. For the tiles, we calculated the anchor points at the different side of the intersected plane related to p^{BD} respectively. These anchor points are removed to avoid intersected into the other ting's roof since they will be at the structure of the other ting to be combined as shown in the right of Fig. 8. The tiles then can be placed at the remaining anchor points by the method described in [4]. After the processing of the ridge and tiles, we can obtain a combined ting.

Corridor & Garden Wall. In Chinese garden architectures, corridors are used to connect the main building, while garden walls surround the whole area. The structure of corridor and garden wall both have platform and roof in gable type, but there are columns and/or wall in corridor and no columns in garden wall. We focus on building the basic single layer and straight corridor/garden wall.

By the width and length from user input parameters, we can obtain a corridor by extending the width of a gable ting [4] and introduce extra columns. Liang and Heh [2] describe that the columns should be placed in the distance of a *room width* along the width. We restrict the user input width in the integer multiple of the room width, so the placement of each column can be easily decided. A garden wall is obtaining by the method of gable roof ting without the columns, but with a wall beneath the roof and along the main ridge, as shown in Fig. 2(e).

Intersected Region Detection. There are three types of intersected region in corridor and garden wall: L-type, T-type, and cross-type [3] as shown in Fig. 9(a), (b), and (c), respectively. We take each corridor or wall as a rectangle projected onto the floor to illustrate the concept.

As the L-type, the two corridors/garden walls will be extended towards the intersected area to cover the hole as shown in the rectangle area on the top-left of Fig. 9(d). In our implementation, we restrict the direction of the corridor and wall along x - or z -axis only to apply an intersection-test method to get the intersection area between every two AABB rectangles as the rectangles shown in the middle row of Fig. 9.

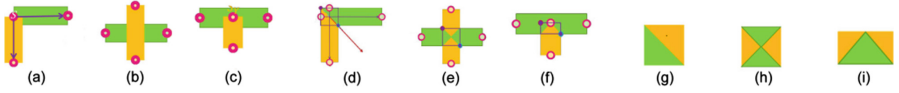


Fig. 9. An illustration of intersection types and processes of corridor and garden wall. (a)~(c): three intersected types: L-, T-, and cross-type. (d)~(f): intersected region detection (with extended region of L-type). (g)~(i): region that roof component (anchor points) to be removed for each type, respectively

Intersection Processing. In the intersected region, we process the intersection in body and roof structures respectively.

Body Structure. For the corridor, the body structure is almost the same with the gable roof ting. The difference is that we have to add extra columns along the width direction with the *room width* as shown in Fig. x. For the garden wall, we construct a 3D mesh beneath the roof and along the main ridge by the thickness of the wall $wall.thickness = \frac{wall.height}{3} + \frac{wall.height-9}{3}$ [1, 16, 17], as shown in Fig. x.

Roof Structure. As mentioned above, the L-type corridors/garden walls will be extended towards the intersected area to cover the hole as shown in Fig. 9(d). The ridges that lie in the intersected area of the L-type intersection are ignored. Then, the roof components that lie in the area of the corner triangle (different color to the original rectangle) are removed as shown in the bottom row of Fig. 9. As the T-type and the cross-type, the process on roof components (anchor points and ridge) who lies in the area of the triangle is the same as those of combined ting. Finally, the corridor/garden wall is obtained.

5 Simplification and Level-of-Detail

The total amount of the polygons in the resultant model is too large to be used in the real-time applications. In this section, we propose simplification and level-of-detail methods to reduce the amount of the polygons while keeping the overall level-of-detail shape of the output 3D architecture models.

5.1 Roof Surface Simplification

For preserving the overall shape of architecture while simplifying its 3D model, we have to take the following information into account.

According to the previous method [4], the PCPs play an important role for deciding the overall shape of a featured architecture, while the components of the roof are placed according to the anchor points. We take advantage of these points by triangulating them to obtain the 3D mesh of whole roof, excluding the ridges. The points we try to triangulate are ordered due to the construction process of the roof frame [4]. Therefore, we can use the order to make the triangulation more efficient.

The order of points we obtain after the roof frame construction process is from p^{Rg} towards p^{EvC} along the eave curve (green line), and from eave curve towards the ridge (orange line) along roof surface curves (cyan lines) shown in the right of Fig. 8. Hence, the points can be triangulated according this order.

5.2 Other Components Simplification

Ridge and ridge tail models are generated by sweeping a complex contour in previous method [4]. The curvature of these components are crucial of a roof's shape, so we have to retain the curvature while perform the simplification simultaneously. To this end, we keep the number of the segment points of them while only replacing the complex contour with a simple rectangle instead when sweeping.

Other components, such as column, purlin, beam and tiebeam, are replaced using low-polygon template models (cylinder or box) to replace the corresponded components. Moreover, we use a rectangular plane to replace balustrade, frieze, and sparrow brace, letting artists to enrich the content using texture.

5.3 Level-of-Detail

The number of polygons is decreased significantly after the simplification process, but we would like to further control the number of triangles to a certain extent. We take advantage of the level-of-detail method. Level-of-detail techniques scale the detail of the 3D objects according to their visual importance within the scene [20].

The level-of-detail method we used is to evenly sample the anchor points before triangulating them with the critical points for maintaining the overall shape of the roof. Therefore, we keep these critical points (Fig. 3) and perform a uniform sampling on the rest anchor points with a sampling rate

$$s = \frac{d}{t} \times i/2 \quad (1)$$

where d is the distance between the camera and the model center, or an adjustable parameter given by user, t is the maximum value of d , and i is the number of segment of the eave curve. That is, we can control the number of polygon by adjusting the parameter d .

6 Results

We have implemented the proposed methods and developed an integrated modeling tool on a PC with a 3.20 GHz Intel Core i5-3470 CPU, 8 GB RAM and an NVIDIA GeForce GTX 550 Ti graphics card using C# and DirectX API.

The left of Fig. 11(a) shows a resultant 3D model of a ting with gable-and-hip roof. The two different column layouts, single-rounding column and double-rounding column, of double-eave structure are shown in the top-left and bottom-left of Fig. 11(c), respectively. The left of Fig. 11(b) shows a three-layer pagoda. It takes less than thirty seconds for a user to create with only three clicks of the keyboard and slightly adjust the control points by mouse.

The resultant 3D models of combined tings in edge- and ridge-aligned with hexagonal and rectangular platform are shown in Fig. 12(a) and (b), respectively, with comparison of the real ones. Figure 12(c) and (d) show the resultant 3D models of the corridors and garden walls, respectively. Note that the bottom-right of the Fig. 12(c) is the top view of the model to show the type clearly. modeling time of the above 3D models can be seen in Table 1.

The proposed simplification and LOD method can extraordinarily decrease the number of polygon while keeping the overall shape of a structure. Figure 10 shows the comparison of polygon count for the original and simplified models using our proposed LOD method. Note that the polygon count of the original model, shown in Fig. 10(a),

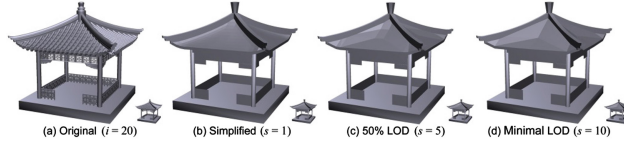


Fig. 10. The comparison between (a) the original detailed 3D model, (b) simplified model, (c) 50% LOD model, and (d) minimal LOD (critical points only).

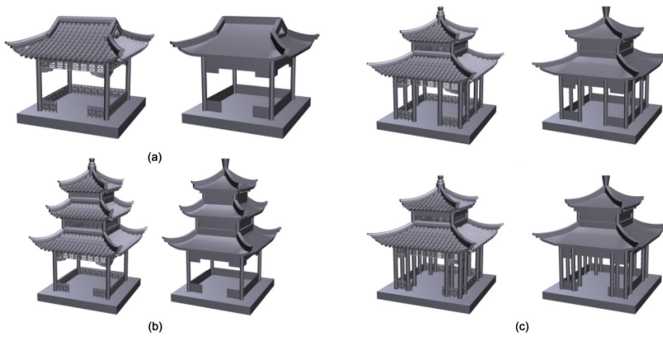


Fig. 11. The resultant models of extended roof types with their simplified 3D models. (a) A ting with gable-and-hip roof (maximum LOD). (b) A three-layer pagoda (minimum LOD). (c) Top: a ting with single-rounding double-layer roof; bottom: a ting with double-rounding double-layer roof (50% LOD).

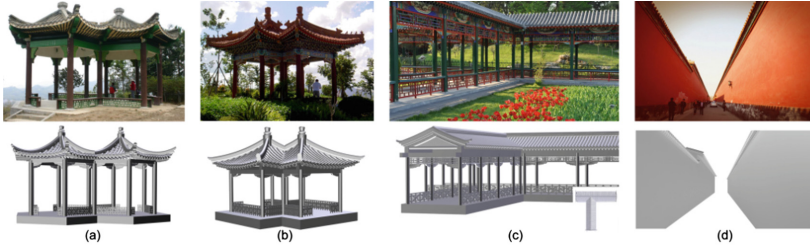


Fig. 12. The comparison of the real extended tings and the 3D models we obtained. (a) An edge-aligned hexagonal combined ting. (b) A ridge-aligned rectangular combined ting. (c) A T-type corridor. (d) Two garden (palace) wall.

is 197,284, while that of the minimal LOD model (critical points only), shown in Fig. 10(d), is down to 1,408, which means 99.3% of the polygons are reduced. Figure 10(b) and (c) are the simplified models of Fig. 10(a) with maximal and 50% LOD, respectively. The small models beside Fig. 10(a) to (d) show that the salience features are almost retained when zoom-out (80% smaller than the original size). The corresponding simplified models of Fig. 11 are shown in the right of the original models of Fig. 11 with maximum, minimum, and 50% LOD, respectively. The polygon count and the LOD parameters of the models we used in this paper are shown in Table 2, with $i = 20$ and $t = 1000$. Note that the simplified 3D models in Fig. 11 are rendered using 3D ExplorationTM with smoothing parameter set to be 40, while those in Fig. 10 are not smooth rendered.

Table 1. The polygon count and the modeling time of the resultant 3D models of extended ting structures

| Model | Polygons | Modeling time |
|--------------|----------|---------------|
| Figure 12(a) | 405,776 | 4m30s |
| Figure 12(b) | 327,548 | 2m27s |
| Figure 12(c) | 608,436 | 2m25s |
| Figure 12(d) | 518,243 | 5m08s |

Table 2. The comparison of the polygon count and the parameters used

| Model | Polygons | d | s |
|--------------------------------|----------|---------|-----|
| Figure 11(a) left | 188,192 | N/A | N/A |
| Figure 11(a) right | 3,296 | 1000 | 1 |
| Figure 11(b) left | 355,620 | N/A | N/A |
| Figure 11(b) right | 3,432 | 119 | 10 |
| Figure 11(c) top-/bottom-left | 296,456 | N/A | N/A |
| Figure 11(c) top-/bottom-right | 2,944 | 514/547 | 5 |
| Figure 10(a) | 197,284 | N/A | N/A |
| Figure 10(b) | 3,248 | 100 | 1 |
| Figure 10(c) | 1,536 | 500 | 5 |
| Figure 10(d) | 1,408 | 1000 | 10 |

7 Conclusion

In this paper, we have extended the previous work [4] to modeling more kinds of featured Chinese architectures such as gable-and-hip roof, double-eave structure, pagoda structure, combined ting, corridor, and garden wall of the Chinese garden. We

combine pyramidal roof structure with gable roof to model the gable-and-hip structure, combine pyramidal and hollow roof to model the double eave structure, and stack several layers of a single ting to model the pagoda structure. Also, we combine the multiple tings in both vertical and horizontal directions to model double-layer, pagoda, and combined ting structure, and dealing with the intersection area to model the corridor and the garden wall. The experimental results show that our approach can effectively obtain similar 3D models to the real architectures in minutes.

The limitations lie on the complex structure of combined ting, such as round-ceiling-square-floor ting and the curved structured corridor. We plan to improve our approach to cover the above types of architecture to enrich our capability of modeling various featured Chinese architectures. Furthermore, we would like to improve the approach for better manipulation, capable of importing customized component models, and taking aid from image(s) for the reconstruction of the existing eastern feature architecture more precisely, intuitively, and semi-automatically.

References

1. Bai, L.-J., Wang, J.-F.: *The Structure of the Official Building in Ching Dynasty* (Ch'ing Tai Guan Shih Jien-ju Go-zao). Publisher of Beijing University of Technology, Beijing (2000)
2. Liang, S.-C., Heh, Z.-Y.: *The Example of the Construction and Computation of the Architecture in Ching Dynasty* (Ch'ing Tai Ying-tsao Tse Li). Wen Hai Foundation for Culture and Education, Taipei (1985)
3. Liu, D.-K.: *The Construction Methods of Ancient Chinese Building* (Chung-kuo Ku Chien-chu Wa-shih Yin-fah). Publisher of Construction Industry of China, Beijing (1993)
4. Huang, C.-Y., Tai, W.-K.: Ting tools: interactive and procedural modeling of Chinese ting. *Vis. Comput.* **29**, 1303–1318 (2012)
5. Ganster, B., Klein, R.: An integrated framework for procedural modeling. In: Sbert, M. (ed.) *Spring Conference on Computer Graphics 2007 (SCCG 2007)*, pp. 150–157. Comenius University, Bratislava (2007)
6. Parish, Y., Müller, P.: Procedural modeling of cities. In: *28th Annual Conference on Computer Graphics and Interactive Techniques*, pp. 301–308 (2001)
7. Prusinkiewicz, P., Hammel, H., Hanan, J., Měch, R.: Visual models of plant development. In: Rozenberg, G., Salomaa, A. (eds.) *Handbook of Formal Languages*, vol. 3. Springer, Heidelberg (1997)
8. Prusinkiewicz, P., Hammel, M., Měch, R., Hanan, J.: The artificial life of plants. In: *SIGGRAPH 1995 Course Notes*, vol. 7, pp. 1–38 (1995)
9. Prusinkiewicz, P., James, M., Měch, R.: Synthetic topiary. In: *SIGGRAPH 1994*, pp. 351–358 (1994)
10. Prusinkiewicz, P., Lindenmayer, A.: *The Algorithmic Beauty of Plants*. Springer, Heidelberg (1990)
11. Wonka, P., Wimmer, M., Sillion, F., Ribarsky, W.: Instant architecture. *ACM Trans. Graph.* **22**(3), 669–677 (2003)
12. Müller, P., Vereenoghe, T., Wonka, P., Paap, I., Van Gool, L.: Procedural 3d reconstruction of puuc building in xkipché, *Eurographics Symposium on Virtual Reality, Archaeology and Cultural Heritage (VAST)*, pp. 139–146 (2006)

13. Müller, P., Wonka, P., Haegler, S., Ulmer, A., Van Gool, L.: Procedural modeling of buildings. *ACM Trans. Graph.* **25**(3), 614–623 (2006)
14. Bokeloh, M., Wand, M., Seidel, H.-P.: A connection between partial symmetry and inverse procedural modeling. *ACM Trans. Graph.* **29**(4), 104:1–104:10 (2010)
15. Chen, X., Kang, S., Xu, Y.-Q., Dorsey, J., Shum, H.-Y.: Sketching reality: realistic interpretation of architectural designs. *ACM Trans. Graph.* **27**(2), 11:1–11:15 (2008)
16. Tian, Y.-F.: *The Construction and Design of Chinese Garden Architecture*. Publisher of Construction Industry of China, China (2008)
17. Wang, S.-D., Ma, S.: *Chinese Garden Architecture*. Publisher of China Meteorological Press, China (2001)
18. Zong, W.-C.: *Atlas of Chinese Garden Architecture*. Publisher of China Book Press, China (1995)
19. Wang, S.-D., Ma, S.: *The Design of Chinese Garden Architecture*. Publisher of Southeast University Press, China (2004)
20. Luebke, D., Reddy, M., Cohen, J., Varshney, A., Watson, B., Huebner, R.: *Level of Detail for 3D Graphics*. Morgan-Kaufmann Inc., Burlington (2003)

Smart Graphics

13th International Symposium, SG 2015, Chengdu,
China, August 26-28, 2015, Revised Selected Papers

Chen, Y.; Christie, M.; Tan, W. (Eds.)

2017, X, 215 p. 122 illus., Softcover

ISBN: 978-3-319-53837-2